Tetrahedron Letters 54 (2013) 1348–1351

Contents lists available at SciVerse ScienceDirect

Tetrahedron Letters

journal homepage: www.elsevier.com/locate/tetlet

Selective and colorimetric fluoride chemosensors containing phenol hydroxyl and 1,3,4-oxadiazole groups

Jiantao Ma, Zhe Li, Yanqing Zong, Yi Men *, Guowen Xing

Beijing Key Laboratory of Energy Conversion and Storage Materials, College of Chemistry, Beijing Normal University, Beijing 100875, China

ARTICLE INFO

Article history:
Received 30 September 2012
Revised 7 December 2012
Accepted 14 December 2012
Available online 9 January 2013

Keywords:
Sensor
F^-
Oxadiazole
Hydrogen bond
Fluorescence

ABSTRACT

Two novel anion sensors, methyl 4-(5-(5-chloro-2-hydroxyphenyl)-1,3,4-oxadiazol-2-yl) benzoate (**L1**) and methyl 4-(5-(2-hydroxyphenyl)-1,3,4-oxadiazol-2-yl) benzoate (**L2**) were reported. Their spectroscopic and colorimetric properties in CH_2Cl_2/CH_3CN (1:2, v/v) solution for F^- sensing were investigated by naked-eye, UV–vis, and fluorescence measurements. Both molecules with coplanar structure possess adjacent phenolic hydroxyl and 1,3,4-oxadiazole units, resulting in a sufficiently strong intramolecular hydrogen bond to hinder the association of most anions, but not F^-, with phenolic hydroxyl hydrogen. They displayed the same color changes from colorless to yellow but different optical shifts upon addition of F^-.

Inorganic anions are crucial for numerous biochemical and environmental processes.[1] Among the various anions, UV–vis and fluorescence sensors for fluoride ion have received much attention due to its duplicitous influence on human health[2] and the environment.[3] However, because $H_2PO_4^-$ and CH_3COO^- possess similar basicity as F^- and easily form hydrogen bonds, only a few of anion sensors are capable of distinguishing fluoride ion effectively from these ions.[4] The achievement of specific optical F^- sensing is still a challenge.

Generally, most fluorescent F^- sensors consist of two parts: a receptor and a chromophore. The former is an ion antenna, typically composed of various better hydrogen-bond donors, such as phenols, pyrroles, imidazoles, and carbazole-based molecules.[5] The latter is capable of converting a test signal into an optical signal that can be detected by the naked eye and simple instrumentation. Among fluorescent materials, heterocyclic ring systems, especially molecules containing 1,3,4-oxadiazole groups, are attracting a great deal of attention because of their excellent electron-acceptor abilities, high thermal stability, and high photoluminescence quantum yields. Oxadiazole-based compounds are promising for highly sensitive ion sensing[6] and have also been studied as electron transporters, emitters for OLED,[7] and optical data storage materials.[8]

We designed and synthesized two novel compounds, **L1** and **L2** (Scheme 1). Both coplanar molecules possess adjacent phenolic hydroxyl and 1,3,4-oxadiazole units, and the resulting intramolecular hydrogen bond is strong enough to hinder the association of most anions, but not F^-, with the phenolic hydroxyl hydrogen. Electron-withdrawing groups, such as –Cl and $–COOCH_3$, are introduced into the molecules to tune the acidity and the hydrogen-bond acceptor abilities of both molecules. Thus, both molecules display highly selective and colorimetric responses to F^-; the addition of F^- created distinct color and fluorescence changes that could be observed by the naked-eye and simple instrumentation.

The response of **L1** to F^- was first investigated by UV–vis spectroscopy (Fig. 1). Adding F^- to free **L1** in CH_2Cl_2/CH_3CN (1:2, v/v) gave rise to a dramatic color change from colorless to yellow, which was accompanied by spectral changes. The shoulder at 294 nm blue shifted to 272 nm, a new broad absorption band formed at 423 nm, and the band at 327 nm ascribed to the π–π^* transition of the oxadiazole group decreased in intensity. In the process, the electron density in **L1** was increased by the addition of F^- because of the hydrogen bond formation between **L1** and F^- and subsequent elimination of the proton in the phenolic hydroxyl group of **L1**, which led to an increase in electron delocalization (Scheme 1). This delocalized π-conjugated bond was energetically higher than that of **L1**, resulting in a red shift of the π–π^* transition[9] from 327 to 423 nm. Thus, the hydrogen bond formation and subsequent deprotonation induced a consistent effect on the UV–vis absorption of **L1**. Two isosbestic points were observed at 279 and 352 nm, respectively, despite the reaction having two steps. The stoichiometry between **L1** and F^- was proved by the fluorescence job plot (411 nm), in which the maximum value appeared at 0.67, giving a sensor/fluoride stoichiometry of 1:2

* Corresponding author.
E-mail address: menyi@bnu.edu.cn (Y. Men).

0040-4039/$ - see front matter © 2013 Elsevier Ltd. All rights reserved.
http://dx.doi.org/10.1016/j.tetlet.2012.12.128

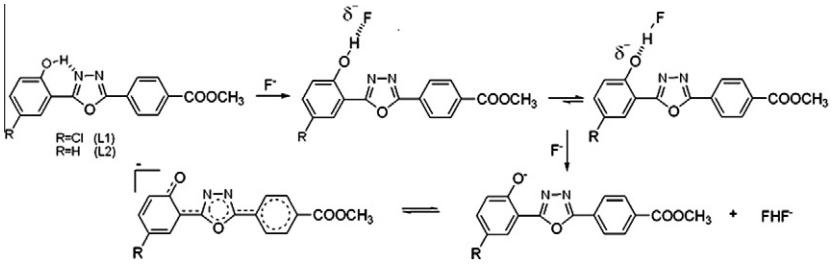

Scheme 1. Sensing behavior of **L1** and **L2** to F^-.

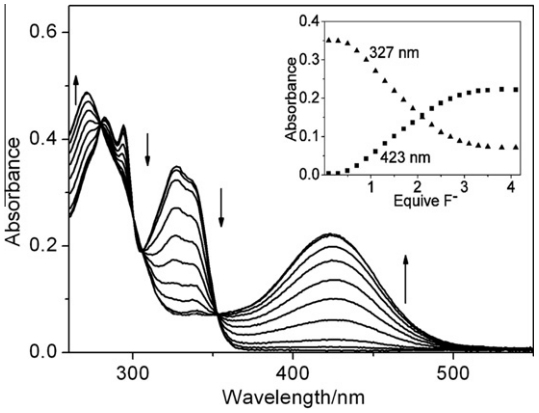

Figure 1. UV–vis absorption spectrum changes of **L1** (1.0×10^{-5} mol L^{-1}) in CH_2Cl_2/CH_3CN (1:2, v/v) upon the addition of F^-. Inset: the absorbance changes at 327 and 423 nm versus $[F^-]/[\mathbf{L1}]$.

(Fig. S1). The absorbance changes at both 327 and 423 nm as a function of the $[F^-]/[\mathbf{L1}]$ ratio were shown in the inset of Figure 1. Calculated after the addition of 3.8 equiv of F^-, corresponding to the end of the reaction, the absorbance ratio ($A_{423\ nm}/A_{327\ nm}$) increased greatly from 0.011 for free **L1** to 3.15 for **L1** with F^-. Importantly, the corresponding spectral and color changes upon the addition of other anions, such as Br^-, I^-, $H_2PO_4^-$, and CH_3COO^-, were quite small (Fig. 2) due to their weak basicity, and the strong intramolecular hydrogen bond of **L1** hindered the association of these anions with the proton of the phenolic hydroxyl. Thus, **L1** can be used as a colorimetric, ratiometric, and highly selective F^- sensor.

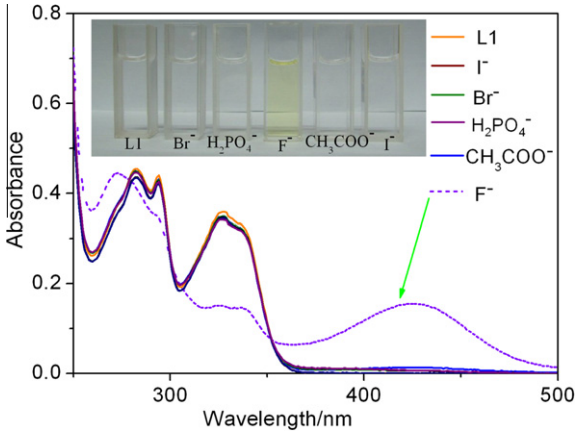

Figure 2. UV–vis absorption spectra changes of **L1** (1.0×10^{-5} mol L^{-1}) in CH_2Cl_2/CH_3CN (1:2, v/v) on the addition of $[Bu_4N]R$ (R = Br^-, I^-, F^-, $H_2PO_4^-$, and CH_3COO^-, 3.8 equiv). Inset: relevant color changes of solution.

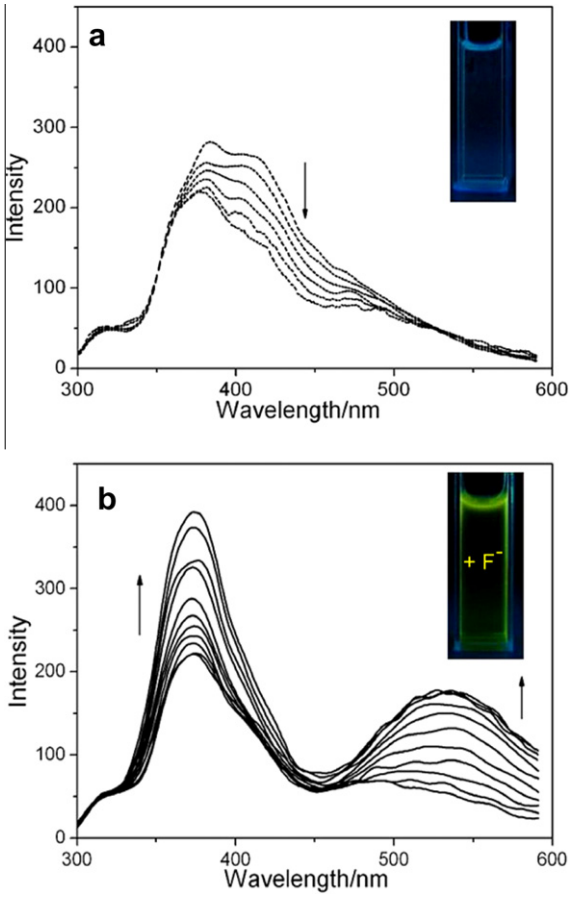

Figure 3. Emission spectra changes of **L1** (1.0×10^{-5} mol L^{-1}) in CH_2Cl_2/CH_3CN (1:2, v/v) upon the addition of F^- (0–3.8 equiv) excited at 270 nm. (a) Dotted line and black arrow: the first fluorescence changes (0–1.9 equiv); (b) Solid line and black arrows: the second fluorescence changes (1.9–3.8 equiv). Inset: fluorescence emission color changes of the **L1** in the absence (a) and presence (b) of F^-.

As shown in Figure 3, **L1** displayed two-step emission changes upon F^- addition. Over the gradual addition of 1.9 equiv of F^-, the emission peak at 411 nm decreased (Fig. 3a) simultaneously with the appearance of a new blue-shift emission peak at 375 nm, which was attributed to the formation of a hydrogen bond between **L1** and F^-. Further addition of F^- led to a gradual increase in the intensity of the new peak at 375 nm and the appearance of a new emission peak at 532 nm (Fig. 3b), which was attributed to the deprotonation of **L1**. The increasingly negative charge density of the phenol oxygen atom promoted the intramolecular charge transfer (ICT)[10] from the phenol oxygen anion to the aromatic rings, which was further enhanced by the –Cl electrophilic group. The intensity of the peak at 532 nm continued to increase until the addition of 3.8 equiv of F^-, after which the peak at 375 nm

continued to grow. Consequently, an obvious fluorescence color change from pale blue to green was observed (Fig. 3, inset), exhibiting light-on behavior and colorimetric F^- sensing. No such spectral changes were detected upon the addition of other anions (Br^-, I^-, $H_2PO_4^-$, and CH_3COO^-).

The above discussion indicates that the process of **L1** sensing F^- actually involved a two-step reaction: hydrogen bond formation and deprotonation. They are attributed to the small radius and the strong ability of F^- to form hydrogen bond and to the high stability of the byproduct, FHF^-. Interestingly, the addition of 4 equiv of water changed the solution color from yellow back to colorless and produced the original absorption spectra. It is clear that the hydrogen bonding interaction existed between **L1** and F^- and was then destroyed by the addition of water. To prove the deprotonation step, [Bu_4N]OH was added, producing the same effect on the UV–vis and fluorescence emission spectra of **L1** as the addition of F^- (Fig. S2).

The sensing mechanism of **L1** was further investigated by ^1H NMR titration experiments in DMSO-d_6 at room temperature (Fig. 4). The signal for –OH proton at 10.65 ppm became undetectable after the addition of 0.4 equiv of F^-, which is attributed to the transformation of the strong hydrogen bonding interaction from –O–H···F^- to –O^-···H–F (Scheme 1). All other peaks shifted upfield upon F^- addition because the increased charge density weakened the deshielding effect of the electronegative groups. The effect on the shift of the H_3–H_5 signals was more than that of the H_1 and H_2 signals, producing a large shift ($\Delta\delta$ = 0.45, 0.60, and 0.74 ppm for H_3, H_4, and H_5, respectively, for 3.8 equiv of F^-). This finding suggests that the electron density is dispersed along the entire molecule through the delocalized π-conjugated bond, which favors the fluorescence emission of the phosphor. The FHF^- peak was located at 16.39 ppm.[11]

The stoichiometry of **L1** and F^- was also determined by the Benesi–Hildebrand equation.[12] As shown in Figure 5, the value of $1/(A-A_0)$ is linearly proportional to $1/[F^-]^2$ (R = 0.997), which indicated that F^- interacted with **L1** in a 2:1 stoichiometry. This result is in agreement with that of the job plot and fluorescence titrations (Fig. S3). The dissociation constant (K) and detection limit (3σ/slope)[13] of **L1** toward F^- were calculated as 2.08×10^9 L^2 mol^{-2} and 5.6×10^{-8} mol L^{-1}, respectively.

Lacking a –Cl, electron-withdrawing group in the phenolic ring, **L2** also exhibited sensitivity to F^-. Upon addition of F^-, the intensities of the absorption bands at 320 and 294 nm gradually decreased while that of the new band at 416 nm gradually increased (Fig. S4), which is similar to the results observed with **L1**. The change in the absorbance ratio ($A_{416\ nm}/A_{320\ nm}$) for **L2**, increasing from 0.003 to 1.621, was lower than that for **L1**.

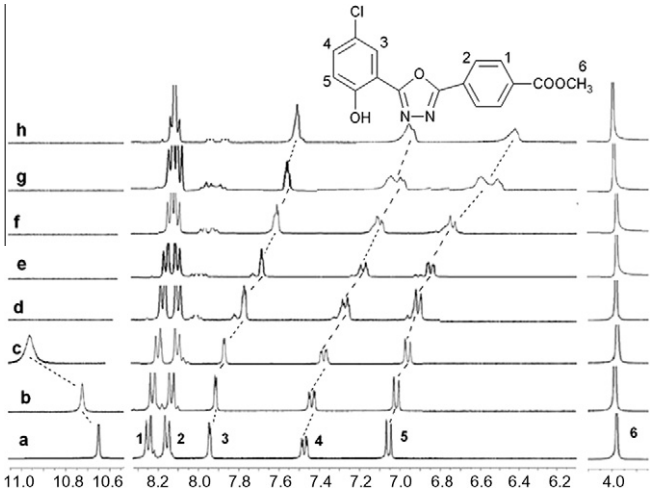

Figure 4. Partial ^1H NMR titration of **L1** in DMSO-d_6 in the absence (a) and the presence of 0.1 equiv; (b) 0.2 equiv; (c) 0.4 equiv; (d) 1.0 equiv; (e) 2.0 equiv; (f) 3.0 equiv; (g) 3.8 equiv; (h) of F^-.

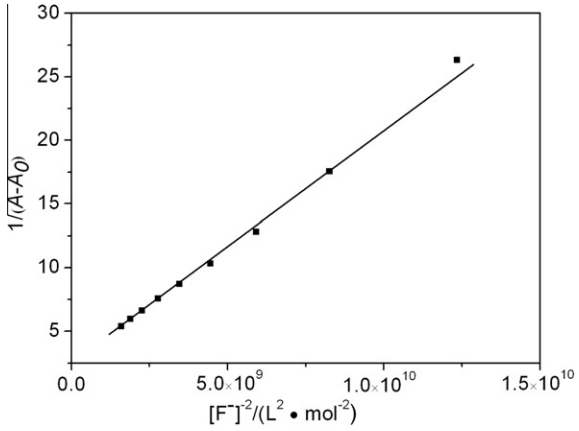

Figure 5. Benesi–Hildebrand plot, determined 1:2 stoichiometry for association between **L1** and F^- by UV–vis titration results (423 nm).

However, **L2** displayed different two-step emission changes from that of **L1** upon the addition of F^- (Fig. S5). During the addition of F^- from 0 to 7 equiv, the emission peak at 411 nm decreased following the appearance of a new blue-shifted emission peak at 386 nm with a shoulder at 399 nm. After 7 equiv of F^-, the peak intensity at 386 nm increased gradually. Similar to the case of **L1**, two emission changes were responsible for this behavior: the hydrogen bond formation of **L2**–F^- and the deprotonation of **L2**. In contrast, no new emission peak was observed at longer wavelengths, even after the addition of excess F^-, which is perhaps because **L2** does not contain a withdrawing group in the phenolic ring, resulting in the negative charge transferring toward the oxadiazole ring. The K and detection limit of **L2** with F^- were determined to be 1.05×10^9 L^2 mol^{-2} and 1.4×10^{-7} mol L^{-1}, respectively. The dissociation constant for the reaction of **L1** with F^- is double that of **L2** and the detection limit is also quite low, which demonstrate that **L1** is a better F^- sensor.

In conclusion, we have designed and developed two novel F^- sensors, **L1** and **L2**. As the effect of electron-withdrawing substituents (–Cl), the solution of **L1** became yellow and fluorescent green color upon the addition of F^-, which can be detected by the naked-eye and optical spectrum, while the solution of **L2** became yellow without any fluorescent color change. Both compounds could detect F^- at 0.01 and 0.1 ppm level concentrations, respectively, displaying a high selectivity and quantitative sensitivity for F^- over Br^-, I^-, $H_2PO_4^-$, and CH_3COO^-.

Acknowledgments

This work was supported by the Key Technologies R&D Program for the 12th Five-Year Plan (2012BAJ24B04-3) of the Ministry of Science and Technology of the People's Republic of China and by the Fundamental Research Funds for the Central Universities, China.

Supplementary data

Supplementary data (experimental and characterization details for compounds **L1** and **L2**, ^1H and ^{13}C NMR spectra, ESI and elemental analysis, changes in the absorption and emission spectra of **L1** upon addition of Bu_4NOH, changes in the absorption and emission spectra of **L2** upon addition of F^-) associated with this article can

be found, in the online version, at http://dx.doi.org/10.1016/j.tetlet.2012.12.128.

References and notes

1. (a) Gale, P. A. *Chem. Commun.* **2011**, *47*, 82–86; (b) Ali, H. D. P.; Kruger, P. E.; Gunnlaugsson, T. *New J. Chem.* **2008**, *32*, 1153–1161; (c) Kim, T. H.; Choi, Y. S.; Sohn, B.; Park, S.; Lyood, W. S.; Lee, T. S. *Chem. Commun.* **2008**, 2364–2366; (d) Peng, X.; Wu, Y.; Fan, J.; Tian, M.; Han, K. *J. Org. Chem.* **2005**, *70*, 10524–10531; (e) Kwak, C. K.; Leeb, C. H.; Leea, T. S. *Tetrahedron Lett.* **2007**, *48*, 7788–7792; (f) Guha, S.; Saha, S. *J. Am. Chem. Soc.* **2010**, *132*, 17674–17677.
2. (a) Dale, T. J.; Rebek, J., Jr. *J. Am. Chem. Soc.* **2006**, *128*, 4500–4501; (b) Cametti, M.; Rissanen, K. *Chem. Commun.* **2009**, 2809–2829; (c) Bassin, E. B.; Wypij, D.; Dai, S.; Li, W.; Tang, Y.; Zhang, Y.; Feng, P. *Appl. Geochem.* **2007**, *22*, 1017–1024; (d) Turner, C. H.; Owan, I.; Brizendine, E. J.; Zhang, W.; Wilson, M. E.; Dunipace, A. J. *Bone* **1996**, *19*, 595–601; (e) Xu, W.; Liu, S.; Zhao, X.; Sun, S.; Cheng, S.; Ma, T.; Sun, H.; Zhao, Q.; Huang, W. *Chem. Eur. J.* **2010**, *16*, 7125–7133.
3. (a) Kubik, S. *Chem. Soc. Rev.* **2010**, *39*, 3648–3663; (b) Meenakshi; Meenakshi, R. C. *J. Hazard. Mater. B* **2006**, *137*, 456–463.
4. (a) Hijji, Y. M.; Bararea, B.; Kennedya, A. P.; Butcherb, R. *Sens. Actuators, B.* **2009**, *136*, 297–302; (b) Kumar, M.; Babu, J. N.; Bhalla, V.; Athwal, N. S. *Supramol. Chem.* **2007**, *19*, 511–516; (c) Li, J. W.; Chen, H.; Lin, H.; Lin, H. *J. Photochem. Photobiol., B* **2009**, *97*, 18–21; (d) Zheng, Z.; Duan, Z.; Zhang, J.; Wang, K. *Sens. Actuators, B* **2012**, *169*, 312–319; (e) Liu, X.; Zhao, Q.; Song, W.; Bu, X. *Chem. Eur. J.* **2012**, *18*, 2806–2811.
5. (a) Wang, Q.; Xie, Y.; Ding, Y.; Li, X.; Zhu, W. *Chem. Commun.* **2010**, *46*, 3669–3671; (b) Zhao, Y.; Zhao, C.; Wu, L.; Zhang, L.; Tung, C.; Pan, Y. *J. Org. Chem.* **2006**, *71*, 2143–2146.
6. Wang, G.; He, Y. *Mater. Lett.* **2009**, *63*, 470–472.
7. (a) Wang, J.; Jabbour, G. E.; Mash, E. A.; Anderson, J.; Zhang, Y.; Lee, P. A.; Armstrong, N. R.; Kippelen, B. *Adv. Mater.* **1999**, *11*, 1266–1269; (b) Jin, R.; Zhang, J. *Chem. Phys.* **2011**, *380*, 17–23; (c) Wang, J.; Wang, R.; Yang, J.; Zheng, Z.; Carducci, M. D.; Cayou, T.; Peyghambarian, N.; Jabbour, G. E. *J. Am. Chem. Soc.* **2001**, *123*, 6179–6180.
8. Liu, Y.; Wang, K.; Huang, G.; Zhu, C.; Tok, E.; Neoh, K. G.; Kang, E. T. *Chem. Mater.* **2009**, *21*, 3391–3399.
9. Men, Y.; Korupoju, S. R.; Kurihara, M.; Mizutani, J.; Nishihara, H. *Chem. Eur. J.* **2005**, *11*, 7322–7327.
10. Wen, Z. C.; Jiang, Y. B. *Tetrahedron* **2004**, *60*, 11109–11115.
11. Wang, H. X.; Wang, D. L.; Wang, Q.; Schalley, C. A. *Org. Biomol. Chem.* **2010**, *8*, 1017–1026.
12. (a) Benesi, H. A.; Hildebrand, J. H. *J. Am. Chem. Soc.* **1949**, 2703–2707; (b) Han, F.; Bao, Y.; Yang, Z.; Fyles, T. M.; Zhao, J. *Chem. Eur. J.* **2007**, *13*, 2880–2892; (c) Chu, Q.; Medvetz, D. A.; Pang, Y. *Chem. Mater.* **2007**, *19*, 6421–6429.
13. Han, Z.; Zhang, X.; Li, Z.; Gong, Y.; Wu, X.; Jin, Z.; He, C.; Jian, L.; Zhang, J.; Shen, G.; Yu, R. *Anal. Chem.* **2010**, *82*, 3108–3113.